**Zeitschrift:** Schweizerische mineralogische und petrographische Mitteilungen = Bulletin suisse de minéralogie et pétrographie

**Band:** 83 (2003)

**Heft:** 1

**Artikel:** Metamorphic evolution and significance of a serpentinized peridotite slice within the Eclogitic Micaschist Complex of the Sesia-Zone (Western Alps - Italy)

**Autor:** Ferraris, Christiano / Compagnoni, Roberto

**DOI:** https://doi.org/10.5169/seals-63131

*Schweizerische Mineralogische und Petrographische Mitteilungen 83, 3–13, 2003*

# Metamorphic evolution and significance of a serpentinized peridotite slice within the Eclogitic Micaschist Complex of the Sesia-Zone (Western Alps – Italy)

*Cristiano Ferraris*[1,*] and *Roberto Compagnoni*[2]

**Abstract**

The petrography, mineral chemistry, and metamorphic evolution of a serpentinized peridotite slice, which occurs within the Eclogitic Micaschist Complex of the Sesia-Lanzo zone, western Alps (Italy), are described and possible tectonic implications are discussed. The ultramafics are mainly foliated serpentinites which preserve, in the central portion, relics of the peridotitic protolith. The relic peridotite includes both orthopyroxene- and olivine-rich layers and consists of olivine, diopsidic clinopyroxene, Cr-bearing chlorite and orthopyroxene porphyroclasts. The latter include olivine, amphibole, and orange-brownish Cr-Mg-Al-rich spinel aggregates, whose spatial arrangement indicates pseudomorphism after a mineral with a perfect cleavage set, most likely chlorite. Based on this interpretation, arisen from both the composition and geometric arrangement of spinel droplets, the host peridotite preserves evidence of a prograde metamorphism from the chlorite- to the spinel-peridotite field, which predates the Alpine polyphase evolution. The study of a rodingite – most likely derived from a gabbro protolith crosscutting the peridotite – which contains a zoned garnet rich in grossular in the core and in almandine in the rim, suggests that an episode of low-T metasomatic alteration occurred prior to the early-Alpine eclogite-facies metamorphism. The presence of this rodingite, which shows the same mineral zoning and evolution as those already described for the nearby meta-ophiolitic ultramafic Lanzo Massif, suggests that the relic peridotite slice belongs to the Piemonte zone. It is thus seen as a sliver derived from the Mesozoic Tethys Ocean that has been tectonically emplaced into the continental crust of the Sesia zone. These data partly support the interpretation of Venturini (1995) and Venturini et al. (1991, 1992, 1994) and indicate that the Eclogitic Micaschist Complex, usually considered as a coherent fragment of Variscan continental crust, is in fact a unit with a more complex internal tectonic setting.

*Keywords:* serpentinized lherzolite, rodingite, Sesia-Zone, Western Alps.

## Introduction

Understanding the geodynamics of high-pressure metamorphic terrains is fundamental to the study of orogenic processes. High-pressure metamorphic assemblages are common in rocks of oceanic affinity that have been exhumed from fossil subduction zones (see e.g. Hermann et al., 2000; Schwartz et al., 2001).

Serpentinites resulting from the hydration of ultramafic rocks frequently surface in convergent geodynamic settings. Recent studies have shown that subduction of serpentinized lithospheric mantle plays a key role in the process because of its dehydration, which provides for a repository to recycle water in the mantle (Ulmer and Trommsdorff, 1995; Schmidt and Poli, 1998), and in the exhumation of high-pressure – low-temperature rocks in subduction zones (Scambelluri et al., 1995; Guillot et al., 2000, 2001; Schwartz et al., 2001).

Eclogite facies metamorphism has been recorded in several units of the western Alps. These units are particularly important in understanding the dynamics of the Alpine orogeny because the time available for the collision, burial, and exhumation cycle is known to be less than 100 Ma. In particular, the Sesia-Lanzo Zone of the western Alps, an extensive unit of the eclogite-bearing continental crust with affinity to the African continent, is well constrained in its metamorphic evolution (Dal Piaz et al., 1972; Compagnoni, 1977; Gosso, 1977; Compagnoni et al., 1977; Lardeaux and Spalla, 1991; Inger et al., 1996; Ruffet et al., 1997; Rubbo et al., 1999), but field evidence and data from relics of its subduction evolution during the closure of the Tethys Ocean have been missing up to now.

[1] Department of Earth Sciences, University of Siena, Via Laterina 8, 53100 Siena, Italy.
[2] Department of Mineralogical and Petrological Sciences, University of Torino, Via V. Caluso 35, 10125 Torino, Italy.
* Present address: Institute of Environmental Science and Engineering (IESE), Nanyang Technological University (NTU), Innovation Center Block 2, Unit 247, 18 Nanyang Drive, Singapore-637723. <cferraris@ntu.edu.sg>

0036-7699/2003/83/3 

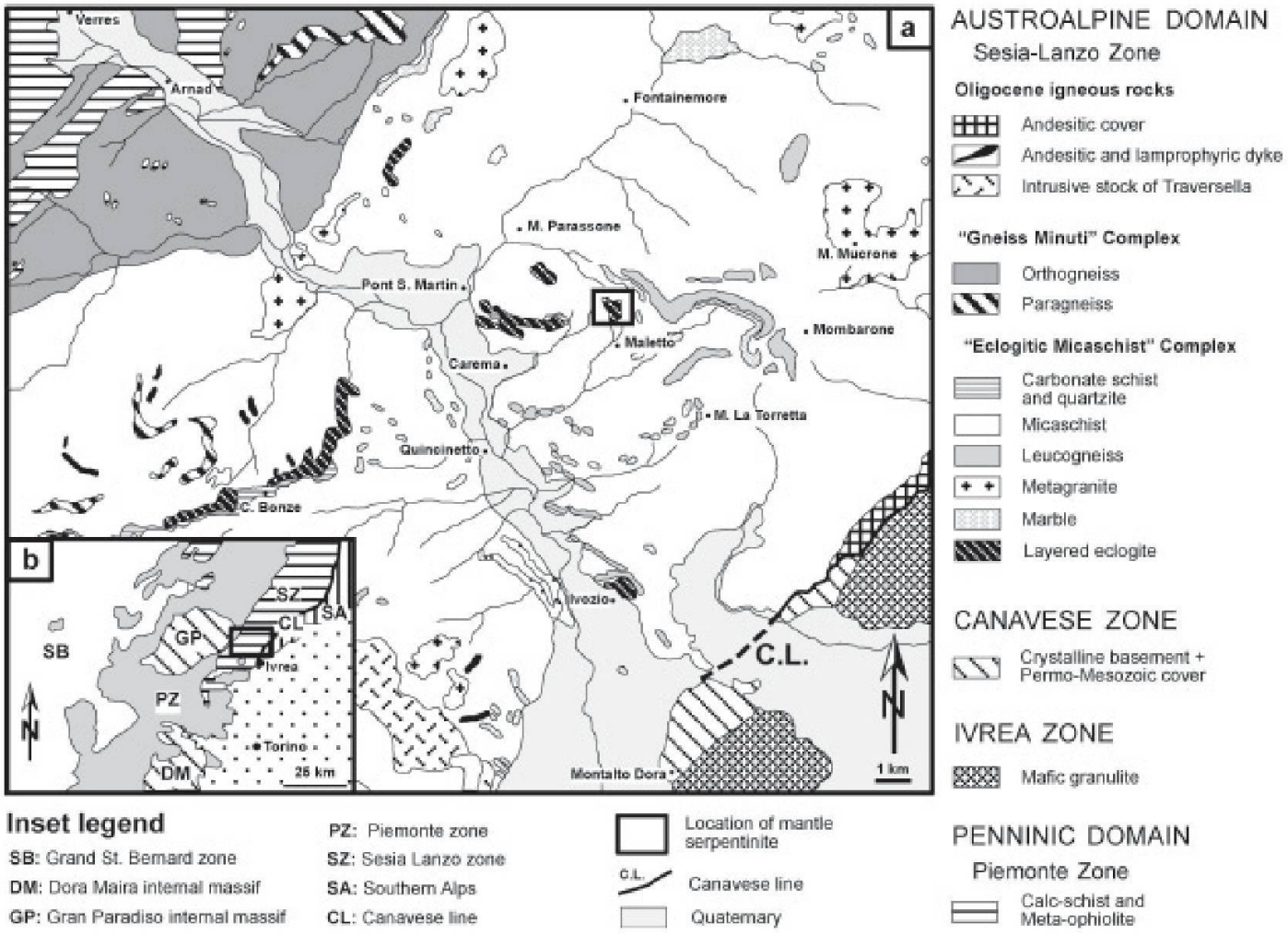


*Fig. 1* (a) Simplified geological map of the central Sesia Zone (modified after Venturini et al., 1994). The inset shows location of Fig. 2. (b) Simplified tectonic sketch map of a portion of the northwestern Alps. The inset shows location of Fig. 1a.

This study focuses on a recently discovered sliver derived from the Mesozoic Tethys ocean and tectonically emplaced into the continental crust of the Sesia-Lanzo Zone. This indicates that the Eclogitic Micaschist Complex, so far considered as a coherent fragment of Variscan continental crust, is really a unit with internal tectonic contacts.

The petrography, mineral chemistry, and metamorphic evolution of a small outcrop of serpentinite containing relics of pre-Alpine peridotite and associated rodingite are described, and possible tectonic implications are discussed.

## Geological setting

The Sesia-Lanzo Zone (SLZ), the internal tectonic unit of the western Alps, together with the Dent Blanche nappe, the Monte Emilius nappe and other smaller outliers, forms the composite Austroalpine system of the western Alps (Carraro et al., 1970) (Fig. 1).

The SLZ is classically subdivided into (Fig. 1), *(i)* the "Eclogitic Micaschist Complex" (EMC), *(ii)* the "Gneiss Minuti Complex" (GMC), and *(iii)* the "Seconda zona diorito-kinzigitica" (IIDK). The three tectonic units consist of a continental basement, composed of Variscan amphibolite-facies rocks intruded by late-Variscan granitoids, that experienced a polyphase tectono-metamorphic reworking during the Alpine orogeny (Dal Piaz et al., 1972; Compagnoni, 1977; Gosso, 1977; Compagnoni et al., 1977; Lardeaux and Spalla, 1991).

The first Alpine metamorphic event attained eclogite-facies conditions in the EMC (Compagnoni, 1977), P–T conditions between eclogite- and epidote blueschist-facies in the GMC (Williams and Compagnoni, 1983), and epidote blueschist-facies conditions at the base of the IIDK.

The peak of the high-pressure (HP), subduction-related, metamorphism has been dated at around 65 Ma ago in the EMC (Inger et al., 1996; Duchêne et al., 1997; Ruffet et al., 1997; Rubatto, 1998; Rubatto et al., 1999). Greenschist-facies

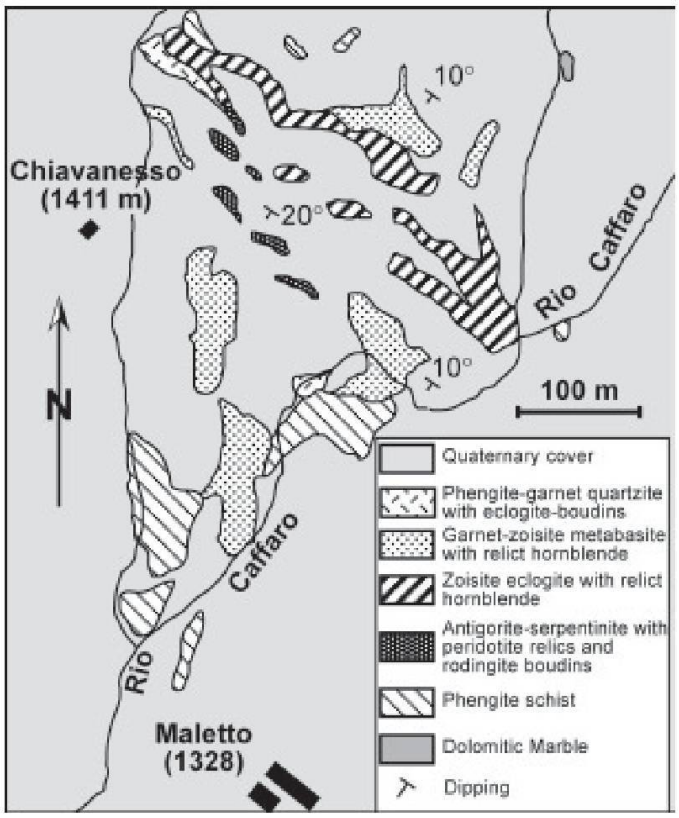


*Fig. 2* Geological map of the ultramafic and associated rocks from the EMC. For location see Fig. 1a.

mineral assemblages characterize the second Alpine metamorphic overprint, post-dating nappe emplacement. This event pervasively obliterated the HP mineral assemblages only in the GMC and in the external EMC, whereas in the other units the overprint is mainly localized along shear zones.

Venturini et al. (1991, 1992, 1994) and Venturini (1995) suggested a new tectono-stratigraphic interpretation for the SLZ. In addition to the polymetamorphic basement characterized by the occurrence of relics of Variscan amphibolite-facies mineral assemblages, they reported a monometamorphic cover complex subdivided into two units: *(i)* the Bonze unit, originally composed of pillow basalts, sediments and gabbro fragments of probable Mesozoic age, and *(ii)* the Scalaro unit, a sequence composed of metacarbonate, quartzite and metapelite of probable Permo-Triassic age. However, a recent geochronological study (U–Pb SHRIMP data on zircon, Rubatto et al. 1999) found that eclogites from the Bonze unit, previously supposed to derive from Tethyan basalts, are HP products of Carboniferous gabbros intruded some 355 Ma ago. These metagabbros are part of the intrusive layered complex, previously recognized in the area (Pognante et al., 1980; Ferraris and Compagnoni, 1997).

The serpentinized peridotite studied occurs within the EMC on the northern wall of the lower Valle d'Aosta, near Maletto place, some 2.5 km ENE from Carema village (UTM coord.: 32TLR10014910). Exposed on the left side of Rio Caffaro between ~1400 and 1475 m altitude, it occurs as a slice, about 170 m long and 10–30 m thick, dipping 20–40° towards the NNE (Fig. 2).

The ultramafic body is sandwiched between banded eclogites, which are surrounded by metasediments of the EMC (Ferraris and Compagnoni, 1997) (Fig. 2). The contact in the hanging wall between ultramafite and metabasites is characterized by the presence of a quartzite layer up to ca. 1 m thick, while a discontinuous dark green layer, a few cm-thick, consisting of coarse-grained amphibole and sparse albite, outlines the footwall contact.

## Petrography

### *Ultramafic rocks*

The ultramafic body is mainly foliated antigorite serpentinite, which preserves relics of the peridotite assemblage in its central portion. These relics show a cm-thick compositional layering, defined by alternating pyroxene- and olivine-rich layers, and a tectonitic fabric. The tectonic fabric is defined by orthopyroxene porphyroclasts up to several cm long, included in a finer-grained matrix, mainly consisting of partially serpentinized olivine.

Microscopically, the relic peridotite consists of orthopyroxene porphyroclasts included in a granoblastic matrix of medium grain-size olivine, chlorite nests, and minor amphibole (Fig. 3a).

*Orthopyroxene* (Opx; abbreviations after Kretz, 1983) occurs either as single crystals with a subgrain structure or as aggregates of deformed crystals; in both cases crystals are of cm-size. Opx porphyroclasts usually show an internal foliation ($S_i$) defined by *olivine* (Ol) and minor clinopyroxene (Fig. 3b); the olivine defining $S_i$ is finer-grained than the one marking the rock foliation ($S_e$). $S_i$ seems concordant with $S_e$ (Fig. 3b). Even in the less retrogressed samples, Ol is partly replaced at the rim by early antigorite and later lizardite in association with magnetite (Figs. 3a and 4). Locally, Opx contains *spinel* (Spl) that occurs in aggregates of elongate, orange-brownish rods 1–2 μm across. Spinel aggregates show a crystal arrangement suggesting pseudomorphism after a mineral with a perfect cleavage system (Fig. 5a).

*Clinopyroxene* (Cpx) usually occurs within the Opx porphyroclasts as prismatic crystals elongated parallel to $S_i$ (Fig. 3b).

Two generations of *amphibole* were recognized: the earlier one (Am 1) occurs as small crystals, about 10 μm across, within orange-brownish

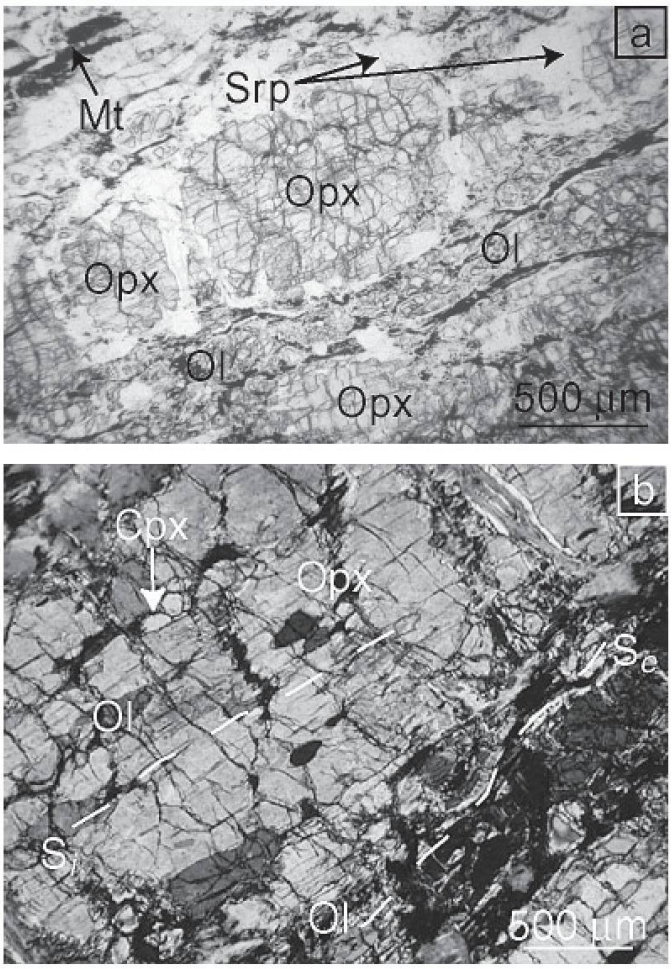


*Fig. 3* Microphotograph of relic peridotite. (a) Orthopyroxene porphyroclasts (Opx) included in a granoblastic matrix of olivine (Ol) partly retrogressed to antigorite (Srp) + magnetite (Mt). (b) Within Opx $S_i$ is defined mostly by olivine grains (Ol); clinopyroxene (Cpx) (arrow) seems concordant with $S_e$ of the matrix (see also Fig. 3a).

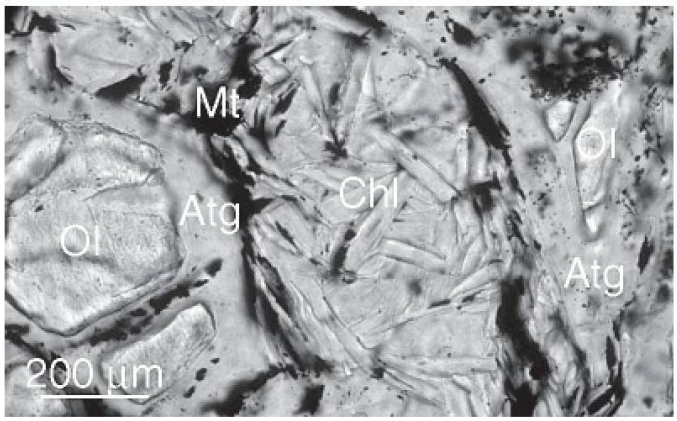


*Fig. 4* Microphotograph of partially serpentinised peridotite. The granoblastic olivine grains (Ol) of the rock matrix are partially retrogressed to Atg + Mt. In the center, an aggregate of randomly oriented chlorite flakes. Plane polarised light (PPL).

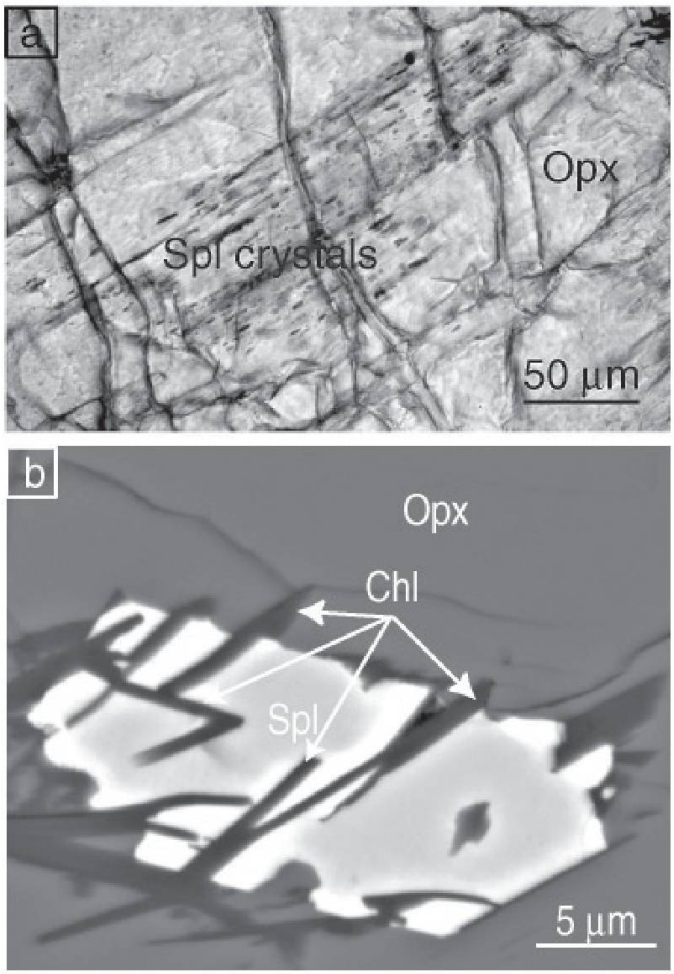


*Fig. 5* (a) Microphotograph of the orange-brownish spinel (Spl) aggregates armored within Opx porphyroclast. Note preferred elongation and spatial arrangement of the spinel aggregate, interpreted as a pseudomorph after Cr-bearing Mg-chlorite. Plane Polarized light. (b) Back scattered image of spinel shows grain zonation; chlorite flakes (Chl) originate by hydrous alteration of spinel.

spinel (Fig. 6a). The later generation (Am 2) occurs in the rock matrix and grew preferentially across the main rock foliation (Fig. 6b).

*Chlorite* (Chl) occurs either as aggregates of randomly oriented flakes associated with magnetite (Fig. 4) or as a retrogression product of the orange-brownish spinel within Opx (Fig. 5b and 6a).

Small, orange crystals of *titanian clinohumite* (Ti-Chu) locally occur in the olivine matrix.

A network of *antigorite* (Atg)- and *lizardite* (Lz) ± *magnetite* (Mt) -veins, up to 1 cm thick, usually cut across the rock. Lizardite veins crosscut those composed of antigorite.

The relics described are usually surrounded by massive serpentinite and foliated antigorite serpentinite. In massive serpentinite, olivine is pseudomorphically replaced by mesh serpentine (Atg) + Mt aggregates, while the "bastite" replaces Opx. The foliated serpentinite locally contains *dolomite* (Dol) and lacks structural and mineral relics of peridotite.

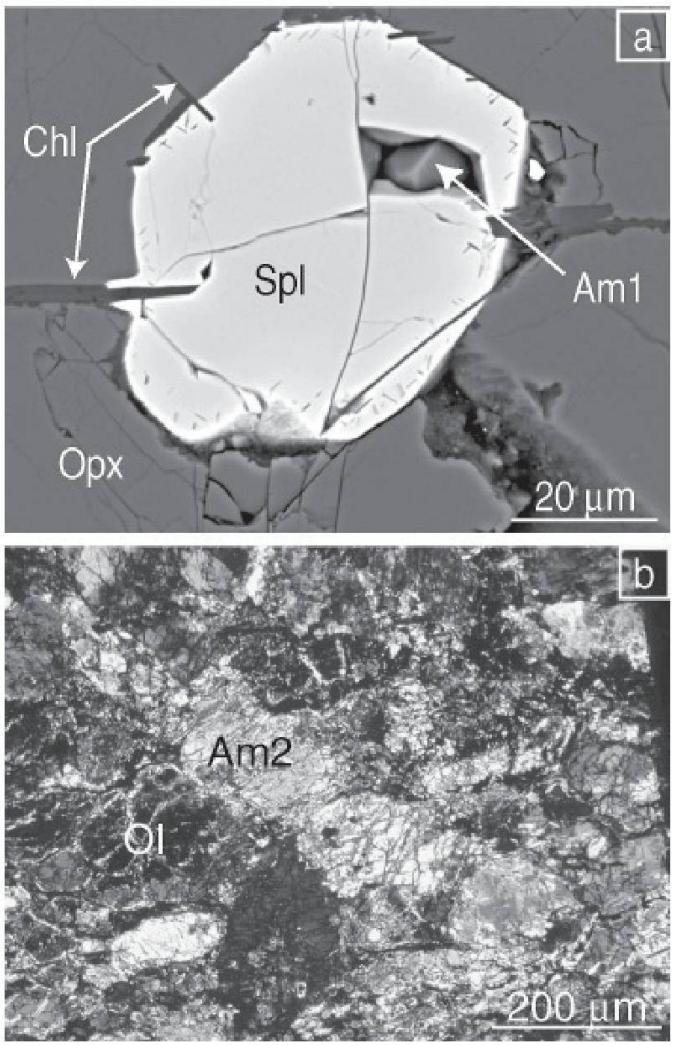


*Fig. 6* (a) Back-scattered image of orange-brownish spinel (see Fig. 5) which includes (Am 1) amphibole. Note retrogressive chlorite flakes (Chl) developed at the expense of spinel. (b) Microphotograph of amphibole (Am 2) in peridotite matrix, overgrowing the rock foliation, defined by olivine and orthopyroxene porphyroclasts. Crossed polarizers.

### *Rodingite*

Boudins of rodingite, a few dm long, are locally found within serpentinite. They are easily distinguished from the host ultramafite by the presence of zoned garnet porphyroblasts up to 1 cm across, embedded in a greenish matrix of *chlorite* and *diopside*.

Garnet (Grt) is zoned, with a colorless core overgrown and partially replaced by a reddish intermediate mantle, which is locally surrounded by a discontinuous colorless rim (Fig. 7). The garnet is poikiloblastic and includes mainly epidote (Ep) in the core and diopside in the reddish mantle.

## Mineral chemistry

Electron microprobe analyses (EMPA) of representative mineral phases from both ultramafite and rodingite were carried out at the Institute of Mineralogy and Petrography, University of Berne, Switzerland, using a Cameca SX50 instrument. Operating conditions were 15 kV and 20 nA for the beam current and about 1 µm electron beam diameter. Absorption and fluorescence corrections were calculated using the PAP routine (Pouchou and Pichoir, 1984). Natural and synthetic oxides and silicates were used as standards.

A set of about 30 points for each of the major minerals was analyzed; for rodingitic garnet, a total of 40 points every about 300 µm along a profile from core to rim, while for spinel and Ti-clinohumite 5 and 7 points were analyzed, respectively. For each phase, the compositions of the analyzed points agrees within ~1% for major elements. The resulting formulas were normalized to 4 O for olivine, 6 O for Cpx, Opx and Dol, 9 (O, OH) for serpentine minerals, 12 O for garnet, 13 (O, OH) for epidote, 18 (O, OH) for Ti-clinohumite, 23 O and

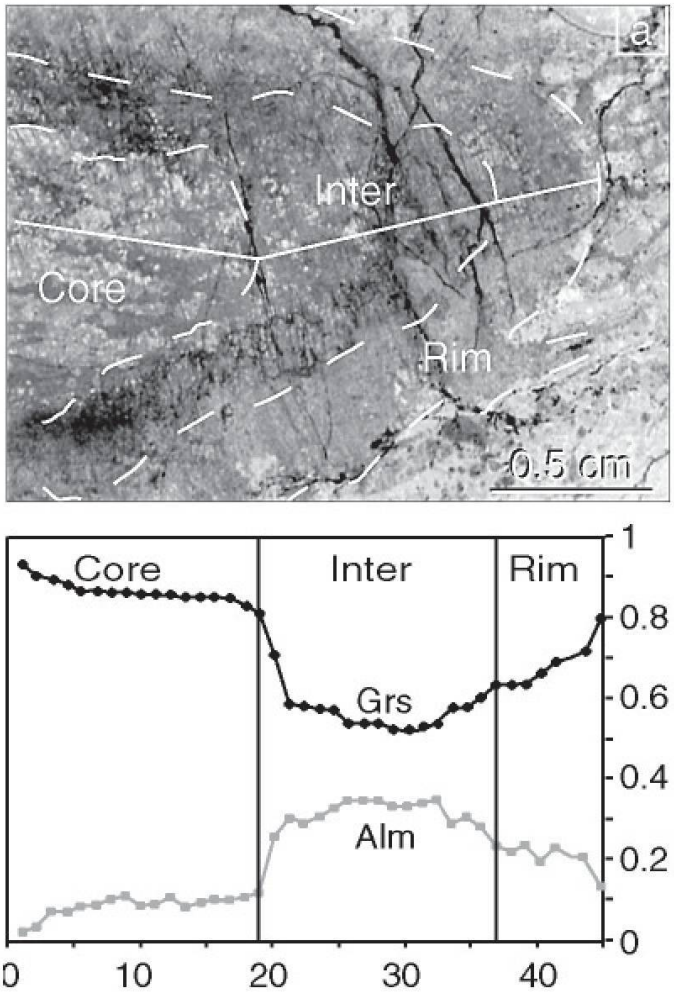


*Fig. 7* Microphotograph of zoned garnet in rodingite. (a) The dashed lines indicate garnet zoning while the white line refers to the profile in Fig. 7b. PPL. (b) Compositional profile (white line in Fig. 7a) across garnet porphyroblast shown in Fig. 7a. Note inverse trends of grossular (Grs) and almandine (Alm) concentrations; abscissa indicates point analyses, ordinate gives mol% of garnet components.

*Table 1* Composition of representative minerals from the partly serpentinized peridotite. (nm: not measured; nc: not calculated). $Fe_2O_3$, $H_2O$, and $CO_2$ contents calculated assuming stoichiometry.

| | Pre-Alpine minerals | | | | | | | Early Alpine minerals | | | | | | Mesoalpine minerals | | | | |
|---|---|---|---|---|---|---|---|---|---|---|---|---|---|---|---|---|---|---|
| | Ol in | Ol out | Opx | Cpx | Am 1 | Spl core | Spl rim | Bastite | Am 2 | Ti-chu | Chl from Spl | Penn. core | Penn. rim | Atg from Ol | Mt | Dol | Atg matrix | Lz veins |
| $SiO_2$ | 41.42 | 41.63 | 57.83 | 55.19 | 54.42 | <0.02 | <0.06 | 41.60 | 53.61 | 38.06 | 34.94 | 34.61 | 34.17 | 42.22 | 1.01 | 0.69 | 41.40 | 39.99 |
| $TiO_2$ | <0.02 | <0.02 | 0.04 | 0.15 | <0.02 | <0.02 | 0.28 | 0.03 | <0.02 | 4.39 | <0.02 | 0.04 | <0.02 | <0.02 | 0.03 | <0.02 | <0.02 | <0.02 |
| $Al_2O_3$ | 0.06 | <0.06 | 0.26 | 0.96 | 3.28 | 35.65 | 2.96 | 0.36 | 1.81 | 0.30 | 14.72 | 13.38 | 12.11 | 0.09 | 0.52 | 0.06 | 0.65 | 5.05 |
| $Fe_2O_3$ | 0.00 | 0.00 | 0.00 | 0.00 | 2.25 | 0.00 | 7.64 | 0.00 | 1.59 | 0.00 | 0.00 | 0.00 | 0.00 | 0.00 | 64.43 | 0.00 | 0.00 | 0.00 |
| FeO | 9.56 | 9.09 | 6.32 | 3.04 | 0.00 | 18.40 | 26.21 | 1.67 | 0.00 | 9.03 | 2.73 | 3.07 | 2.66 | 1.91 | 31.44 | 0.49 | 3.33 | 2.48 |
| MnO | 0.10 | 0.15 | 0.17 | 0.05 | <0.02 | <0.02 | <0.02 | 0.19 | 0.09 | 0.15 | 0.06 | <0.02 | <0.02 | <0.02 | 0.12 | 0.25 | 0.21 | 0.09 |
| MgO | 48.31 | 48.63 | 35.19 | 17.90 | 22.66 | 12.58 | 4.24 | 41.36 | 26.59 | 45.13 | 33.46 | 33.64 | 33.93 | 41.33 | 2.23 | 23.02 | 39.68 | 37.93 |
| NiO | 0.43 | 0.39 | nm | nm | nm | <0.02 | <0.02 | <0.02 | nm | nm | 0.27 | <0.02 | <0.02 | <0.02 | <0.02 | nm | <0.02 | <0.02 |
| ZnO | 0.08 | 0.06 | nm | nm | nm | <0.02 | <0.02 | nm | nm | nm | 0.19 | nm | nm | nm | nm | nm | nm | nm |
| $Cr_2O_3$ | <0.03 | <0.03 | <0.03 | 0.16 | 2.20 | 33.45 | 59.12 | 0.09 | <0.03 | <0.03 | 1.77 | <0.03 | 3.40 | <0.03 | 0.10 | <0.03 | 0.13 | 0.81 |
| CaO | <0.02 | <0.02 | 0.23 | 22.17 | 12.94 | 0.07 | 0.16 | 0.08 | 14.01 | <0.02 | <0.02 | <0.02 | <0.02 | <0.02 | 0.16 | 30.29 | 0.03 | 0.03 |
| $Na_2O$ | nm | nm | nm | 0.26 | <0.03 | nm | nm | <0.03 | <0.03 | nm | <0.03 | <0.03 | <0.03 | 0.06 | nm | nm | <0.03 | <0.03 |
| $K_2O$ | nm | nm | nm | <0.03 | <0.03 | nm | nm | <0.03 | <0.03 | nm | <0.03 | <0.03 | 0.12 | <0.03 | nm | nm | <0.03 | <0.03 |
| $H_2O$ | 0.00 | 0.00 | 0.00 | 0.00 | 2.20 | 0.00 | 0.00 | 14.51 | 2.22 | 2.88 | 11.88 | 15.27 | 13.58 | 14.51 | 0.00 | 0.83 | 14.69 | 13.71 |
| $CO_2$ | 0.00 | 0.00 | 0.00 | 0.00 | 0.00 | 0.00 | 0.00 | 0.00 | 0.00 | 0.00 | 0.00 | 0.00 | 0.00 | 0.00 | 0.00 | 44.37 | 0.00 | 0.00 |
| Total | 99.99 | 99.98 | 100.04 | 99.88 | 99.99 | 100.11 | 100.60 | 99.92 | 99.97 | 99.94 | 100.02 | 100.07 | 100.01 | 100.15 | 100.04 | 100.00 | 99.93 | 100.10 |
| | | | | | | | | | | | | | | | | | | |
| Si | 1.01 | 1.00 | 1.99 | 2.00 | 7.41 | 0.00 | 0.00 | 1.91 | 7.37 | 4.08 | 6.61 | 6.45 | 6.37 | 1.94 | 0.31 | 0.02 | 1.98 | 1.85 |
| Ti | 0.00 | 0.00 | 0.00 | 0.00 | 0.00 | 0.00 | 0.06 | 0.00 | 0.00 | 0.35 | 0.00 | 0.00 | 0.00 | 0.00 | 0.01 | 0.00 | 0.00 | 0.00 |
| $Al^{IV}$ | 0.00 | 0.00 | 0.00 | 0.00 | 0.53 | 9.82 | 0.99 | 0.00 | 0.29 | 0.00 | 1.39 | 1.55 | 1.63 | 0.00 | 0.00 | 0.00 | 0.00 | 0.15 |
| $Al^{VI}$ | 0.00 | 0.00 | 0.01 | 0.04 | 0.00 | 0.00 | 0.00 | 0.02 | 0.00 | 0.04 | 1.80 | 1.61 | 1.32 | 0.00 | 0.18 | 0.00 | 0.01 | 0.12 |
| $Fe^{3+}$ | 0.00 | 0.00 | 0.01 | 0.00 | 0.23 | 0.00 | 1.63 | 0.00 | 0.16 | 0.00 | 0.00 | 0.00 | 0.00 | 0.00 | 14.68 | 0.00 | 0.00 | 0.00 |
| $Fe^{2+}$ | 0.19 | 0.17 | 0.17 | 0.09 | 0.00 | 3.60 | 6.22 | 0.06 | 0.00 | 0.81 | 0.46 | 0.47 | 0.40 | 0.07 | 7.96 | 0.01 | 0.04 | 0.09 |
| Mn | 0.00 | 0.00 | 0.00 | 0.00 | 0.00 | 0.00 | 0.00 | 0.01 | 0.01 | 0.01 | 0.00 | 0.00 | 0.00 | 0.00 | 0.04 | 0.00 | 0.00 | 0.00 |
| Mg | 1.79 | 1.80 | 1.80 | 0.97 | 4.60 | 4.38 | 1.79 | 2.84 | 5.45 | 7.21 | 9.46 | 9.63 | 9.34 | 2.83 | 1.00 | 1.07 | 2.84 | 2.62 |
| Ni | 0.01 | 0.01 | nc | nc | nc | 0.00 | 0.00 | 0.00 | nc | nc | 0.00 | 0.00 | 0.00 | 0.00 | 0.00 | nc | 0.00 | 0.00 |
| Zn | 0.00 | 0.00 | nc | nc | nc | 0.00 | nc | nc | nc | nc | 0.00 | nc | nc | nc | nc | nc | nc | nc |
| Cr | 0.00 | 0.00 | 0.00 | 0.00 | 0.24 | 6.18 | 13.26 | 0.00 | 0.00 | 0.00 | 0.00 | 0.00 | 0.21 | 0.00 | 0.05 | 0.00 | 0.00 | 0.03 |
| | | | | | | | | | | | | | | | | | | |
| Ca | 0.00 | 0.00 | 0.01 | 0.86 | 1.89 | 0.02 | 0.05 | 0.00 | 2.06 | 0.00 | 0.00 | 0.00 | 0.00 | 0.00 | 0.05 | 1.01 | 0.00 | 0.00 |
| Na | nc | nc | nc | 0.02 | 0.00 | nc | nc | 0.00 | 0.00 | nc | 0.00 | 0.00 | 0.00 | 0.01 | nc | nc | 0.00 | 0.00 |
| K | nc | nc | nc | 0.00 | 0.00 | nc | nc | 0.00 | 0.00 | nc | 0.00 | 0.00 | 0.07 | 0.00 | nc | nc | 0.00 | 0.00 |
| OH | 0.00 | 0.00 | 0.00 | 0.00 | 2.00 | 0.00 | 0.00 | 4.45 | 2.04 | 2.06 | 15.04 | 16.50 | 17.52 | 4.39 | 0.00 | 0.17 | 4.28 | 4.24 |
| C | 0.00 | 0.00 | 0.00 | 0.00 | 0.00 | 0.00 | 0.00 | 0.00 | 0.00 | 0.00 | 0.00 | 0.00 | 0.00 | 0.00 | 0.00 | 1.89 | 0.00 | 0.00 |

13 cations + (K + Na + Ca) for amphiboles, 24 O for magnetite and spinel, and 36 (O, OH) for chlorites. For spinel, the $Fe_2O_3$ content was calculated assuming stoichiometry (Droop, 1987). The average relative percentage errors (2σ, %) are: 0.6 for $SiO_2$, 6.2 for $TiO_2$, 3.8 for $Cr_2O_3$, 1.2 for $Al_2O_3$, 2.8 for FeO, 8.0 for NiO, 8.2 for ZnO, 20.4 for MnO, 1.0 for MgO, 1.2 for CaO, 4.2 for $Na_2O$, and 10.0 for $K_2O$.

### *Ultramafic rocks*

*Orthopyroxene* is $En_{90}Fs_{10}$ (Fig. 8) with very low Ca, Al and Mn contents (Table 1); minor CaO (locally up to 0.23 wt%) and $Al_2O_3$ (up to 0.26 wt%) might be due to the presence of micro- to nanometer exsolution lamellae of clinopyroxene or, more likely of amphibole.

*Olivine* defining $S_i$ in orthopyroxene has an average composition $Fo_{91}Fa_9$ (Fig. 8) and a slightly, but statistically significant, higher average content of NiO (up to 0.43 wt%: Table 1) than olivine defining $S_e$ (0.39 wt%: Table 1) with an average composition $Fo_{92}Fa_8$ (Fig. 8).

*Clinopyroxene* is $En_{52}Wo_{43}Fs_5$ (Fig. 8), with a $Mg/Fe^{2+}$ ratio consistent with associated olivine and orthopyroxene.

Small *amphibole* grains included in orange-brownish spinel (Am 1) are tremolitic hornblende, whereas *amphibole* (Am 2) cutting across the main rock foliation, is Mg-hornblende (Table 1).

The orange-brownish *spinel* included in Opx is zoned (Fig. 5b), with a picotite core $(Mg_{.55}Fe^{2+}_{.45})(Al_{.61}Cr_{.39})_2O_4$ rimmed by chromite $(Mg_{.20}Fe^{2+}_{.80})(Cr_{.88}Fe^{3+}_{.11}Ti_{.01})_2O_4$ (Table 1).

*Ti-clinohumite* shows a relatively high Ti content (up to 0.35 a.p.f.u.: Table 1).

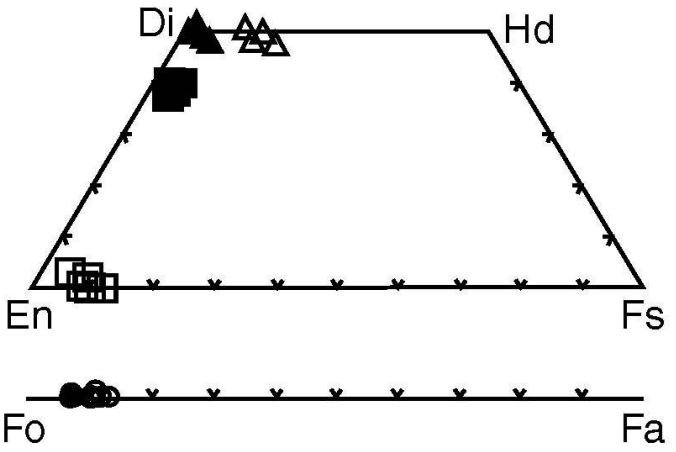


*Fig. 8* Compositions of olivine and pyroxenes from partly serpentinized peridotite and included rodingite. *Peridotite.* Filled circles—olivine defining $S_i$ within Opx porphyroclasts. Open circles—Ol defining $S_e$. Open squares—Opx porphyroclasts. Filled squares—Cpx. *Rodingite.* Filled triangles—Cpx included in garnet. Open triangles—Cpx included in chlorite matrix.

*Chlorite* in the matrix is a zoned penninite, with significant Cr in the rim (up to 0.21 a.p.f.u.: Table 1). Chlorite derived from the alteration of orange-brownish spinel within Opx porphyroclasts (Figs. 5b and 6a) shows lower Cr-contents compared to the rim of the matrix penninite, but higher contents of Al, Ni, Zn, and Mn (Table 1).

Among *serpentine minerals*, Atg in the "bastite" and in pseudomorphs after Ol are chemically very similar: the former is slightly higher in Al, Mn, Cr, and Ca, while Atg in foliated serpentinite has consistently higher FeO contents (about 3.3 wt%: Table 1). Late vein lizardite is systematically higher in Al and Cr than Atg (Table 1).

*Magnetite* coexisting with serpentine minerals (Figs. 3a and 4) has small but significant amounts of Mg, Al, Mn, Cr and Ca (Table 1).

### *Rodingite*

In rodingite, zoned *garnet* is almost pure grossular with an average composition $Grss_{94}Alm_2Sps_2Adr_2$ in the core; the mantle is Fe-rich grossular $Grs_{52}Alm_{34}Prp_7Sps_5Adr_2$, the rim is $Grs_{81}Alm_{13}Sps_6$ (Fig. 7; Table 2).

*Epidote* included in garnet cores is zoned with composition gradually changing from $Zo_{90}Ep_{10}$ in the core towards $Zo_{73}Ep_{27}$ in the rim (Table 2).

*Clinopyroxene* included in intermediate and rim portions of garnet is diopside with mean composition $En_{47}Wo_{48}Fs_5$. Clinopyroxene in the rodingite matrix is similar, but has a higher ferrosilite component ($En_{41}Wo_{48}Fs_{11}$) (Fig. 8; Table 2).

*Chlorite* associated to the matrix diopside is clinochlore (Table 2).

## Metamorphic evolution

In the ultramafic rock, preserved as inclusions within the Opx porphyroclasts, the oldest recognized minerals are spinel (containing Am 1), clinopyroxene, and olivine.

The peculiar geometric arrangement of the spinel aggregates (Fig. 5a) suggests that they derive from the breakdown of a precursor, the nature of which may be tentatively inferred from the shape and chemical composition of the pseudomorphs. The shape indicates a parent mineral with a perfect cleavage, such as a sheet silicate, while the chemical composition suggests a former silicate consisting mainly of Cr, Mg and Al. Due to the relatively simple mineralogy of the ultramafics, the most likely precursor phase is *Cr-rich Mg-chlorite* which is stable over a wide range of P–T conditions (Mysen et al., 1998). If this interpretation is correct, the earliest inferred mineral as-

*Table 2* Composition of representative minerals from the rodingite (nm: not measured; nc: not calculated). $Fe_2O_3$, and $H_2O$ contents calculated assuming stoichiometry. (nm: not measured; nc: not calculated).

| | Pre-Alpine minerals | | | | Alpine minerals | | |
|---|---|---|---|---|---|---|---|
| | Grt core | Zo in Grt | Ep in Grt | Chl | Grt rim | Cpx in Grt | Cpx in matrix |
| $SiO_2$ | 39.49 | 39.25 | 38.92 | 31.39 | 39.53 | 54.89 | 54.94 |
| $TiO_2$ | 0.03 | 0.13 | 0.09 | 0.05 | 0.12 | 0.03 | <0.02 |
| $Al_2O_3$ | 22.25 | 31.99 | 29.84 | 17.74 | 20.28 | 0.17 | 0.74 |
| $Fe_2O_3$ | 0.78 | 2.29 | 4.72 | 0.00 | 0.67 | 0.00 | 0.00 |
| FeO | 1.07 | 0.00 | 0.00 | 6.84 | 16.05 | 2.67 | 5.99 |
| MnO | 0.98 | <0.02 | <0.02 | 0.08 | 1.93 | 0.19 | 0.18 |
| MgO | <0.02 | 0.05 | <0.02 | 29.76 | 1.21 | 16.90 | 13.57 |
| $Cr_2O_3$ | <0.03 | <0.03 | <0.03 | <0.03 | <0.03 | <0.03 | <0.03 |
| CaO | 35.27 | 24.21 | 24.33 | 0.04 | 20.30 | 25.03 | 24.49 |
| $Na_2O$ | nm | <0.03 | <0.03 | 0.03 | nm | <0.03 | <0.03 |
| $K_2O$ | nm | <0.03 | <0.03 | <0.03 | nm | <0.03 | <0.03 |
| $H_2O$ | 0.00 | 1.95 | 1.83 | 14.17 | 0.00 | 0.00 | 0.00 |
| Total | 99.87 | 99.87 | 99.75 | 100.10 | 100.09 | 99.88 | 99.92 |
| Si | 2.98 | 2.99 | 3.02 | 5.89 | 3.03 | 2.00 | 2.01 |
| Ti | 0.00 | 0.01 | 0.00 | 0.01 | 0.07 | 0.00 | 0.00 |
| $Al^{IV}$ | 0.01 | 0.01 | 0.00 | 2.10 | 0.00 | 0.00 | 0.00 |
| $Al^{VI}$ | 1.97 | 2.89 | 2.73 | 3.93 | 1.88 | 0.01 | 0.03 |
| $Fe^{3+}$ | 0.04 | 0.10 | 0.27 | 0.00 | 0.04 | 0.00 | 0.00 |
| $Fe^{2+}$ | 0.07 | 0.00 | 0.00 | 1.07 | 1.06 | 0.08 | 0.19 |
| Mn | 0.06 | 0.00 | 0.00 | 0.01 | 0.13 | 0.01 | 0.01 |
| Mg | 0.00 | 0.00 | 0.00 | 8.33 | 0.14 | 0.92 | 0.75 |
| Cr | 0.00 | 0.00 | 0.00 | 0.00 | 0.00 | 0.00 | 0.00 |
| Ca | 2.87 | 1.99 | 1.94 | 0.01 | 1.71 | 0.98 | 0.98 |
| Na | nc | 0.00 | 0.00 | 0.01 | nc | 0.00 | 0.00 |
| K | nc | 0.00 | 0.00 | 0.00 | nc | 0.00 | 0.00 |
| OH | 0.00 | 1.00 | 1.00 | 17.75 | 0.00 | 0.00 | 0.00 |

semblage should have been Ol + Chl + Opx + Cpx + Am 1, which suggests metamorphic conditions within the *(amphibole-) chlorite-peridotite* stability field. During prograde metamorphism, chlorite would then have been converted to spinel by a dehydration reaction such as: Chl → Opx + Ol + Spl + $H_2O$. As proposed by Schmidt and Poli (1998), this assemblage is consistent with a hydrated peridotite system stable at temperatures no lower than 650 °C at 0.5 GPa and no higher than about 850 °C for pressure of 2 GPa.

A next step of the metamorphic evolution may be inferred by combining the petrologic information derived from both ultramafic rocks and rodingite. The patchy distribution of metamorphic minerals in rodingite may reflect the coarse-grained structure of the protolith, most likely a gabbro dyke, whose plagioclase and clinopyroxene have been replaced by epidote and diopside aggregates, respectively. Within rodingite the presence of zoned garnet, ranging in composition from almost pure grossular in the core to almandine-rich in the mantle and to almandine-bearing grossular in the rim, suggests a three-stage evolution. The grossular core composition, where garnet is associated with zoisite and epidote, is typical of rodingites and suggests relatively low-P (and T) conditions of formation. This stage most likely occurred during rodingitization connected to ocean-floor serpentinization of peridotite. The significant increase in the almandine content in the garnet mantle suggests a new metamorphic event, characterized by a significant increase in P (and T). Finally, the grossular-rich rim composition suggests a further metamorphic event, characterized by lower-P (and possibly T) conditions.

Garnet with similar composition and zoning has been described by Rösli (1988) from a rodingitized gabbro dyke cutting across partly serpentinized peridotites of the nearby Ultramafic Lanzo Massif. The author interpreted the garnet zoning, ranging from almost pure grossular in the core, to grossular with up to ca. 35 mol% almandine component in the rim, as evidence for a two stage rodingitization process: she related the first stage to a low-grade, most likely oceanic, peridotite serpentinization; the second stage was attributed to serpentinization during the early-Alpine high-pressure orogenic metamorphism. Ocean-floor alteration was further supported by a Pb, Sr, O and H stable isotope study by Rösli et al. (1991), which yielded evidence of a two-stage alteration process

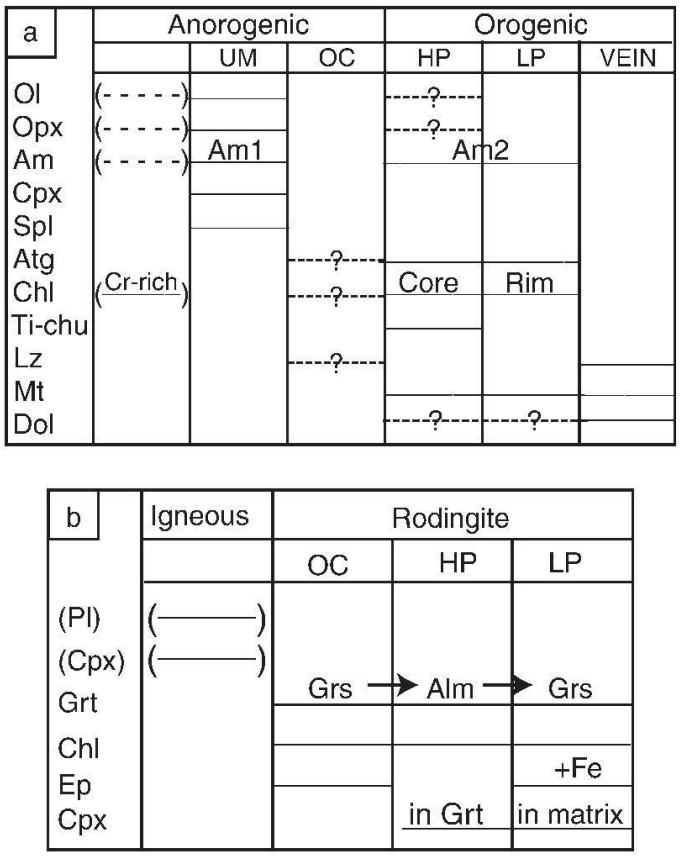


*Fig. 9* (a) Metamorphic evolution of serpentinized peridotite. (b) Metamorphic evolution of rodingite. *Symbols:* UM—Pre-Alpine Upper mantle assemblage. OC—Oceanic assemblage. HP—Alpine high-pressure eclogite-facies assemblage. LP—Alpine low-pressure greenschist-facies assemblage.

of the igneous gabbro protolith: the first alteration process showed interaction "with more or less pure sea water" (p. 138). This event of hydrothermal alteration took place in an oceanic environment and predated the Alpine orogenic history.

In the host ultramafics, such a hydrothermal stage is not recorded, most likely because it has been obliterated by the later tectono-metamorphic evolution. However, the HP event post-dating the hydrothermal alteration is well visible due to the occurrence of the assemblage Ol + Cpx + Chl + Atg + Ti-Chu, which indicates metamorphic conditions of 500–600 °C for pressures in excess of 1.2–1.3 GPa (Evans and Trommsdorff, 1978; Medaris and Carswell, 1990). These conditions are typical of the early-Alpine eclogite-facies metamorphism, characteristic of the EMC. In particular, the presence of Ti-clinohumite is noteworthy, since it systematically occurs all over the ultramafics of the internal Piemonte Zone, characterized by an early-Alpine eclogite-facies metamorphic overprint. The orthopyroxene porphyroclasts are therefore considered to be relics of the thermal climax assemblage, which escaped the retrogression reaction: Opx + Ol + $H_2O \rightarrow$ Atg.

The next metamorphic event is recorded in the ultramafics by the Atg + Mt (± Chl) assemblage and in rodingite by the presence of the discontinuous grossular-rich rim in zoned garnet (see above). The metamorphic conditions of this event are consistent with a low-pressure greenschist-facies late-orogenic event, widespread all over the internal western Alps.

The latest event recognized is characterized by the alteration of olivine to vein lizardite.

On the grounds of the microstructural relationships from both the serpentinized peridotite and the enclosed rodingite, the following tectonometamorphic history, which includes at least 6 stages (Fig. 9), is thus envisaged.

*Stage 1: (amphibole)-chlorite-peridotite facies stage.*
*Stage 2: amphibole-spinel-peridotite facies stage.*
*Stage 3: oceanic hydrothermal stage.*
*Stage 4: early-Alpine eclogite-facies stage.*
*Stage 5: late-Alpine greenschist-facies stage.*
*Stage 6: very-low-grade metamorphic stage.*

## Discussion

Taking into consideration the geology and petrology of both the continent-derived Sesia zone and the ocean-derived Piemonte zone, the following tentative geodynamic reconstruction may be envisaged for the history of the studied ultramafite.

The first two metamorphic stages (Stages 1 and 2) recognized, which are characterized by relatively high T conditions coupled with decompression, may indicate upper mantle conditions predating the Alpine orogeny and leading to the opening of the Mesozoic Tethys Ocean. It is interesting to note that the early chlorite-peridotite facies stage has never been reported from the mantle-derived ultramafics of the Piemonte zone, which are characterized by a decompression evolution from the spinel- to the plagioclase-peridotite-facies fields (e.g. Nicolas, 1966).

The hydrothermal stage (Stage 3) is suggestive of geodynamic conditions, where the upper mantle ultramafics were exposed on the floor of the Tethys Ocean. This scenario, also inferred on the basis of the petrology of ultramafic (Boudier, 1971) and mafic (Rösli, 1988) rocks from the nearby Lanzo Massif, is largely accepted also on the grounds of stratigraphic data on the ocean floor of the Mesozoic Tethys derived from the study of ophiolites of eastern Liguria and the Apennines, which escaped Alpine tectono-metamorphic reworking (e.g. Cortesogno and Haccard, 1984; Lagabrielle and Cannat, 1990).

The eclogite-facies stage (Stage 4) is consistent with the subduction of continental and oceanic crust, which accompanied and followed the closure of the Tethys Ocean and the continental collision between the European and the Adriatic plates (see e.g.: Desmons et al., 1999b). It is interesting to note that eclogitic conditions estimated for the studied ultramafics are consistent with those inferred for the enclosing Eclogitic Micaschist Complex of the Sesia Zone (see e.g. Compagnoni, 1977).

The less pervasive greenschist-facies stage (Stage 5), which is locally observed also in the other lithologies of the Eclogitic Micaschist Complex, corresponds to the second low-P metamorphic event of the Alpine orogeny, which is widespread all across the internal western Alps and marks the rise of the isotherms in response to crustal thickening (e.g. Desmons et al., 1999a).

The very low-grade metamorphic stage (Stage 6) might correspond to the latest isostatic movements and cooling mainly connected to erosion.

## Conclusions

An ultramafic body exposed on the left side of Val d'Aosta, within the Eclogitic Micaschist Complex of the Sesia Zone (Fig. 1 and 2), is interpreted to be a slice of a partly serpentinized upper mantle peridotite most likely derived from the Tethys ocean, as are other ultramafics of the Piemonte Zone. This conclusion is based on petrological data derived from both the ultramafics and enclosed rodingite. A polyphase evolution is suggested, comparable to that of the nearby Lanzo massif. In particular, the tectonitic origin of the ultramafics and the presence of rodingite boudins rules out a close relation with the serpentinized cumulus peridotite of the nearby locality of Ivozio (Pognante et al., 1980), which belongs to a mafic layered complex, emplaced into the Sesia basement about 355 Ma ago and metamorphosed under quartz-eclogite-facies conditions at about 65 Ma ago (Rubatto et al., 1999). By contrast, the ultramafics studied here are considered as an ophiolitic slice, derived from the Tethys Ocean floor and tectonically inserted into the continental crust of the Sesia zone during the Alpine orogeny. Its exotic origin is also supported by the tectonic contacts above and below, towards other lithologies of the Sesia zone. The ultramafic slice has been juxtaposed to the Sesia continental rocks following oceanic hydrothermal alteration, but prior to the eclogite-facies metamorphism dated at ~65 Ma (Rubatto et al., 1999). The same chronological conclusion has been drawn from the study of slices of Sesia rocks within the serpentinized upper mantle ultramafics of the Lanzo massif exposed in the Balangero asbestos mine (Sandrone et al., 1986).

In conclusion, the studied serpentinized peridotite is a tectonic slice of meta-ophiolite introduced into the continental Sesia basement at an early stage of the Alpine orogeny. Since the studied ultramafite is exposed not far from a lithostratigraphic sequence with Mn-bearing quartzite described by Venturini et al. (1994) and Venturini (1995), it is possible that this cover sequence is also exotic to the EMC and may derive from the Tethys ocean as well.

## Acknowledgements

The authors are indebted to G. Filippini, Servizi Tecnici di Prevenzione of Regione Piemonte, for drawing their attention to the presence of serpentinite in the internal Sesia Zone, and to G. Venturini for useful discussions and joint excursions in contiguous areas. Helpful discussions with L. Morten and G. Piccardo are greatly appreciated. The careful and constructive review of Othmar Müntener and of an anonymous referee significantly improved the manuscript. Electron-microprobe analyses, carried out at the Institute of Mineralogy and Petrography, University of Berne, were supported by Schweizerischer Nationalfonds (Credit 21-26579.89). Financial support from CNR, Institute of Geosciences and Earth Resources, Section of Turin, and MIUR is acknowledged.

## References

Boudier, F. (1971): Minéraux serpentineux extraits de péridotites serpentinisées des Alpes Occidentales. *Contrib. Mineral. Petrol.* **33**, 331–345.

Carraro, F., Dal Piaz, G.V. and Sacchi, R. (1970): Serie di Valpelline e II$^a$ Zona Diorito-Kinzigitica sono i relitti di un ricoprimento proveniente dalla zona Ivrea-Verbano. *Mem. Soc. Geol. It.* **9**, 197–224.

Compagnoni, R. (1977): The Sesia Lanzo zone: high-pressure low-temperature metamorphism in the Austroalpine continental margin. *Rend. Soc. Ital. Mineral. Petrol.* **33**, 335–374.

Compagnoni, R., Dal Piaz, G.V., Hunziker, J.C., Gosso G., Lombardo, B. and Williams, P.F. (1977): The Sesia Lanzo zone: a slice of continental crust with alpine high pressure low temperature assemblages in the western Italian Alps. *Rend. Soc. Ital. Mineral. Petrol.* **33**, 281–334.

Cortesogno, L. and Haccard, D. (1984): Note illustrative alla carta geologica della Zona Sestri-Voltaggio. *Mem. Soc. Geol. It.* **28**, 115–120.

Dal Piaz, G.V., Hunziker, J.C. and Martinotti, G. (1972): La Zona Sesia Lanzo e l'evoluzione tettonico-metamorfica delle Alpi Nord occidentali interne. *Mem. Soc. Geol. It.* **11**, 433–460.

Desmons, J., Aprahamian, J., Compagnoni, R., Cortesogno, L. and Frey, M. (1999a): Alpine metamorphism of the Western Alps: I. Middle to high T/P metamorphism. *Schweiz. Mineral. Petrogr. Mitt.* **79**, 89–110.

Desmons, J., Compagnoni, R. and Cortesogno, L. (1999b): Alpine metamorphism of the Western Alps: II.

High-P/T and related pre-greenschist metamorphism. *Schweiz. Mineral. Petrogr. Mitt.* **79**, 111–134.

Droop, G.T.R. (1987): A general equation for estimating $Fe^{3+}$ concentrations in ferromagnesian silicates and oxides from microprobe analyses, using stoichiometric criteria. *Mineral. Mag.* **51**, 431–435.

Duchêne, S., Blichert-Toft, J., Luais, B., Télouk, P., Lardeaux, J.-M. and Albarède, F. (1997): The Lu-Hf dating of garnets and the ages of the Alpine high-pressure metamorphism. *Nature* **387**, 586–589.

Evans, B.W. and Trommsdorff, V. (1978): Petrogenesis of garnet lherzolite, Cima di Gagnone, Lepontine Alps. *Earth Planet. Sci. Lett.* **40**, 415–424.

Ferraris, C. and Compagnoni, R. (1997): Petrology and significance of serpentinised ultramafics discovered in the Sesia zone, Northeast of Carema, lower Val d'Aosta, Western Alps. *Quaderni di Geodinamica Alpina e Quaternaria* **4**, 49–50 (Abstract).

Gosso, G. (1977): Metamorphic evolution and fold history in the eclogitic micaschists of the Gressoney valley (Sesia-Lanzo Zone, western Alps). *Rend. Soc. Ital. Mineral. Petrol.* **33**, 389–407.

Guillot, S., Hattori, K.H., de Sigoyer, J. (2000): Mantle wedge serpentinization and exhumation of eclogites: insights from Eastern Ladakh, Northwest Himalaya. *Geology* **28**, 199–238.

Guillot, S., Hattori, K. H., de Sigoyer, J., Nägler, T. Auzende, A.L. (2001): Evidence of hydration of the mantle wedge and its role in the exhumation of eclogites. *Earth Planet. Sci. Lett.* **193**, 115–127.

Hermann, J., Müntener, O. and Scambelluri, M. (2000): The importance of serpentine mylonites for subduction and exhumation of oceanic crust. *Tectonophysics* **327**, 225–238.

Kretz, R. (1983): Symbols for rock-forming minerals. *Am. Mineral.* **68**, 277–279.

Inger, S., Ramsbotham, W., Cliff, R.A., Rex, D.C. (1996): Metamorphic evolution of the Sesia-Lanzo Zone, Western Alps: time constraints from multi-system geochronology. *Contrib. Mineral. Petrol.* **126**, 152–168.

Lagabrielle, Y. and Cannat, M. (1990): Alpine Jurassic opholites resemble the modern central Atlantic basement. *Geology* **18**, 319–322.

Lardeaux, J-M. and Spalla, M.I. (1991): From granulites to eclogites in the Sesia Zone (Italian Western Alps): a record of the opening and closure of the Piedmont Ocean. *J. Metamorphic Geol.* **9**, 35–59.

Medaris, L.G. and Carswell, D.A. (1990): The petrogenesis of Mg-Cr garnet peridotites in European metamorphic belts. In: Carswell, D.A. (ed.): Eclogite Facies Rocks. Blackie, Glasgow and London, 260–290.

Mysen, B.O., Ulmer, P., Konzett, J. and Schmidt, M.W. (1998): The upper mantle near convergent plate boundaries. In: Russel, J.H. (ed.): Ultrahigh-Pressure Mineralogy: Physics and Chemistry of the Earth's Deep Interior. M.S.A., *Rev. Mineral.* **37**, 97–138.

Nicolas, A. (1966): Le complexe Ophiolites-Schistes lustrés entre Dora-Maira et Gran Paradis (Alpes piémontaises). Tectonique et métamorphisme. Etude pétrochimique des roches vertes et de leur minéraux entre Dora-Maira et Gran Paradis (Alpes Piémontaises). PhD Thesis, Grenoble, 299 pp.

Pognante, U., Compagnoni, R. and Gosso, G. (1980): Micro-mesostructural relationships in the continental eclogitic rocks of the Sesia Lanzo zone (Italian western Alps): a record of a subduction cycle. *Rend. Soc. Ital. Mineral. Petrol.* **36**, 169–186.

Pouchou, J.L. and Pichoir, F. (1984): Un nouveau modèle de calcul pour la microanalyse quantitative par spectrométrie de rayon-X. Partie I: Application à l'analyse d'échantillons homogènes. *La Recherche Aérospatiale* **3**, 167–192.

Rösli, U.E. (1988): Geochemische und mineralogische Untersuchungen an Metarodingiten. Dr. nat. sci. Thesis Nr. 8589, ETH Zürich, unpubl., 261 pp.

Rösli, U., Hoernes, S., Köppel, V. (1991): Isotope data of metarodingites and associated rocks from the mafic complexes. *Schweiz. Mineral. Petrogr. Mitt.* **71**, 125–141.

Rubatto, D. (1998): Dating of pre-Alpine magmatism, Jurassic ophiolites and Alpine subductions in the Western Alps. Dr. nat. sci. Thesis Nr. 12620, ETH Zürich, unpubl., 185 pp.

Rubatto, D., Gebauer, D. and Compagnoni, R. (1999): Dating of eclogite-facies zircons: the age of Alpine metamorphism in the Sesia-Lanzo Zone (Western Alps). *Earth Planet. Sci. Lett.* **167**, 141–158.

Rubbo, M., Borghi, A. and Compagnoni, R. (1999): Thermodynamic analysis of garnet growth zoning in eclogite facies granodiorite from M. Mucrone, Sesia Zone, Western Italian Alps. *Contrib. Mineral. Petrol.* **137**, 289–303.

Ruffet, G., Gruau, G., Ballèvre, M., Féraud, G. and Philippot, P. (1997): Rb–Sr and $^{40}Ar$–$^{39}Ar$ laser probe dating of high-pressure phengites from the Sesia zone (Western Alps): underscoring of excess argon and new age constraints of the high-pressure metamorphism. *Chem. Geol.* **141**, 1–18.

Sandrone, R., Leardi, L., Rossetti, P. and Compagnoni, R. (1986): P–T conditions for the eclogitic re-equilibration of the metaophiolites from Val d'Ala di Lanzo (internal Piemontese Zone, Western Alps). *J. Metamorphic Geol.* **4**, 161–178.

Scambelluri, M., Müntener, O., Hermann, J., Piccardo, G.B. and Trommsdorff, V. (1995): Subduction of water in the mantle: history of an Alpine peridotite. *Geology* **23**, 459–462.

Schmidt, M.W. and Poli, S. (1998): Experimentally based water budgets for dehydrating slabs and consequences for arc magma generation. *Earth Planet. Sci. Lett.* **163**, 361–379.

Schwartz, S., Allemand, P. and Guillot, S. (2001): Numerical model of effect of serpentinites on the exhumation of eclogitic rocks: insights from the Monviso ophiolitic massif (Western Alps). *Tectonophysics* **342**, 193–206.

Ulmer, P. and Trommsdorff, V. (1995): Serpentine stability to mantle depths and subduction-related magmatism. *Science* **268**, 858–861.

Venturini, G., Martinotti, G. and Hunziker, J.C. (1991): The protoliths of the "Eclogitic Micaschists" in the lower Aosta Valley (Sesia Lanzo Zone, Western Alps). *Mem. Soc. Geol. It.* **43**, 347–359.

Venturini, G. and Hunziker, J.C. (1992): Geology and geochronology of the central part of the Sesia Lanzo Zone: the state of the art. Géologie Alpine, série spec., Résumés et Colloques, Univ. Grenoble 1, 102–103.

Venturini, G., Martinotti, G., Armando, G., Barbero, M. and Hunziker, J.C. (1994): The central Sesia-Lanzo zone (Western Alps); new field observations and lithostratigraphic subdivisions. *Schweiz. Mineral. Petrogr. Mitt.* **74**, 111–121.

Venturini, G., (1995): Geology, geochemistry and geochronology of the inner central Sesia Zone (Western Alps). *Mém. Géol. (Lausanne)* **25**, 1–148.

Williams, P.F. and Compagnoni, R. (1983): Deformation and metamorphism in the Bard area of the Sesia Lanzo Zone, Western Alps, during subduction and uplift. *J. Metamorphic Geol.* **1**, 117–140.

Received 28 August 2001
Accepted in revised form 15 April 2003
Editorial handling: M. Engi